# Different basal levels of CaMKII phosphorylated at Thr$^{286/287}$ at nociceptive and low-threshold primary afferent synapses

Max Larsson and Jonas Broman

Department of Experimental Medical Science, Division for Neuroscience,
Lund University, BMC F10, SE-221 84 Lund, Sweden

Corresponding author:
Max Larsson
Department of Experimental Medical Science, BMC F10, SE-221 84 Lund, Sweden
Fax: +46-46-222 45 46
E-mail: max.larsson@mphy.lu.se

No. of pages: 57
No. of figures: 10
No. of tables: 3
No. of words in manuscript: 10 749
No. of words in Abstract: 246
No. of words in Introduction: 489

Abbreviated title: Autophosphorylated CaMKII in the dorsal horn

Keywords: pain; hyperalgesia; electron microscopy; rat

## Abstract

Postsynaptic autophosphorylation of $Ca^{2+}$/calmodulin-dependent protein kinase II (CaMKII) at $Thr^{286/287}$ is crucial for the induction of long-term potentiation at many glutamatergic synapses and has also been implicated in the persistence of synaptic potentiation. However, the availability of CaMKII phosphorylated at $Thr^{286/287}$ at individual glutamatergic synapses *in vivo* is unclear. We used postembedding immunogold labeling to quantitatively analyze the ultrastructural localization of CaMKII phosphorylated at $Thr^{286/287}$ (pCaMKII) at synapses formed by presumed nociceptive and low-threshold mechanosensitive primary afferent nerve endings in laminae I–IV of rat spinal cord. Immunogold labeling was enriched in the postsynaptic densities of such synapses, consistent with observations in preembedding immunoperoxidase stained dorsal horn. Presynaptic axoplasm also exhibited sparse immunogold labeling, in peptidergic terminals partly associated with dense core vesicles. Analysis of single or serial pCaMKII immunolabeled sections indicated that the large majority of synapses formed either by presumed peptidergic or non-peptidergic nociceptive primary afferent terminals in laminae I–II of the spinal cord, or by presumed low-threshold mechanosensitive primary afferent terminals in laminae IIi–IV, contained pCaMKII in their postsynaptic density. However, the postsynaptic levels of pCaMKII immunolabeling at low-treshold primary afferent synapses were only ~50% of those at nociceptive synapses. These results suggest that constitutively autophosphorylated CaMKII in the postsynaptic density is a common characteristic of glutamatergic synapses, thus potentially contributing to maintenance of synaptic efficacy. Furthermore, pCaMKII appears to be differentially regulated between high- and low-threshold primary afferent synapses, possibly reflecting different susceptibility to synaptic plasticity between these afferent pathways.

## Introduction

$Ca^{2+}$/calmodulin-dependent protein kinase II (CaMKII) is well-established as a key enzyme in the induction of NMDA receptor-dependent long-term potentiation (LTP) (Lisman *et al.*, 2002). Following the large postsynaptic $Ca^{2+}$ influx that may occur during strong synaptic activation, CaMKII is rapidly translocated to the postsynaptic density (PSD) or presumed postsynaptic sites (Strack *et al.*, 1997; Shen & Meyer, 1999; Dosemeci *et al.*, 2001; Gleason *et al.*, 2003). This translocation is accompanied by autophosphorylation of the kinase at $Thr^{286}$ (CaMKIIα) or $Thr^{287}$ (other isoforms) (Fukunaga *et al.*, 1995; Barria *et al.*, 1997; Ouyang *et al.*, 1997; Strack *et al.*, 1997; Dosemeci *et al.*, 2002). CaMKII thus phosphorylated (pCaMKII) may subsequently, by triggering phosphorylation and recruitment of postsynaptic AMPA receptors, mediate the early phase of LTP (Barria *et al.*, 1997; Derkach *et al.*, 1999; Hayashi *et al.*, 2000; Lee *et al.*, 2000; Poncer *et al.*, 2002). In addition to the role of CaMKII in LTP induction, persistent postsynaptic presence of pCaMKII has been proposed to be responsible for the ability of LTP to be maintained despite turnover of receptors and other postsynaptic proteins, including CaMKII itself (Lisman & Zhabotinsky, 2001). If this is the case, and if in a population of synapses most have been potentiated from a nascent state by an NMDA receptor-dependent LTP-like mechanism, one would expect that most PSDs in this synaptic population contain pCaMKII. However, earlier studies have not addressed this issue, nor whether synaptic populations with different pre- and/or postsynaptic characteristics differ with respect to the amount of pCaMKII within their PSDs.

Hyperalgesia, the enhanced sensation of painful stimuli, may involve central sensitization of neurons in the superficial dorsal horn of the spinal cord. As primary afferent synapses are glutamatergic (Broman *et al.*, 1993; Valtschanoff *et al.*, 1994;

Larsson *et al.*, 2001; Todd *et al.*, 2003; Alvarez *et al.*, 2004), and central sensitization is NMDA receptor-dependent (Woolf & Salter, 2000; South *et al.*, 2003), this sensitization has been hypothesized to involve mechanisms similar to those underlying hippocampal NMDA receptor-dependent LTP (Sandkühler, 2000; Willis, 2002; Ji et al., 2003). Indeed, numerous studies have demonstrated induction of LTP in dorsal horn neurons by primary afferent stimulation (Randic *et al.*, 1993; Svendsen *et al.*, 1997; Sandkühler & Liu, 1998; Vikman *et al.*, 2001; Ikeda *et al.*, 2003). Furthermore, capsaicin-induced or neuropathic hyperalgesia in rodents has been shown to be associated with increased autophosphorylation of CaMKII in the spinal cord (Fang *et al.*, 2002; Garry *et al.*, 2003; Galan *et al.*, 2004). However, the loci of CaMKII autophosphorylation in the spinal cord, at cellular and subcellular levels, have not been established. For example, the extent to which a constitutive phosphorylation of CaMKII occurs at different populations of primary afferent synapse is unknown. The aim of this study was therefore to investigate the ultrastructural localization of pCaMKII in identified primary afferent synapses in laminae I–IV of the dorsal horn of rats which had not been subject to experimental noxious stimulation.

## Materials and methods

*Animals and surgery*

Adult male Sprague-Dawley rats (~300 g) were anesthetized with sodium pentobarbital (50 mg/kg i.p.), followed by rapid fixation by transcardial perfusion with phosphate-buffered saline (PBS, 300 mOsm, 20–30 s) and 4% paraformaldehyde and 0.1% glutaraldehyde in PBS (~1 l, 30 min). In seven rats used for control experiments, prefixation rinsing was done with PBS containing (four rats) or not containing (three rats) 3 mM lidocaine (Sigma). In these groups of animal, prefixation rinsing was varied between 30 s and 90 s. Following perfusion, the L4 and L5 segments of the spinal cord were removed from each rat. Care was taken not to inflict any noxious stimulation of the hindlimbs prior to fixation. For slice and western blot experiments, non-anesthetized rats were decapitated prior to extraction of spinal cord tissue. Experimental procedures were in accordance with institutional guidelines and were approved by the Animal Care and Use Committee of Malmö-Lund.

*Preparation of tissue from perfusion fixed animals*

For immunoperoxidase labeling, transverse sections (50 μm) of L4 were cut on a Vibratome and processed for pCaMKII immunolabeling as described below.

Lumbar spinal cord sections (40 μm) from the rats perfused with or without 3 mM lidocaine in the rinsing buffer were cut on a freezing microtome prior to immunofluorescent staining of pCaMKII.

For postembedding immunogold labeling, transverse sections (250 μm) of caudal L4 and rostral L5 were cut on a Vibratome. The dorsal parts of the spinal cord sections were cut out and cryoprotected in graded glycerol solutions (30 min each in 10%, 20% and 30%, then overnight in 30%). The sections were plunged into liquid

propane (–180ºC) in a Leica CPC cryofixation system and freeze-substituted in 1% uranyl acetate in absolute methanol at –90ºC for 35 h using Leica AFS freeze-substitution equipment. The temperature was then raised (5ºC/h) to –45ºC and the sections rinsed four times in methanol and infiltrated in graded solutions of Lowicryl HM20 (Electron Microscopy Sciences, Fort Washington, PA) and methanol (2 h each in 1:1, 2:1, 1:0 and then 1:0 overnight). The infiltrated sections were polymerized with ultraviolet light for 30 h at –45ºC, and, following a rise at 5ºC/h, for 40 h at 0ºC. The tissue blocks were trimmed with a razor blade to include major parts of the dorsal horn. Serial ultrathin (~80 nm) sections were then cut and placed on Pioloform-coated slot nickel grids (one or three sections per grid).

*Immunoperoxidase labeling*

Tissue sections were incubated sequentially in: 1% $NaBH_4$ in PBS, 30 min; PBS, 3×5 min; graded solutions of ethanol in PBS in order to enhance antibody permeation [5 min each in 10%, 25%, 45%, 25%, 10% (Carlton & Hayes, 1989)]; PBS, 4×5 min; normal swine serum 1:30 and 0.5% bovine serum albumin in PBS (blocking solution), 1 h; anti-pCaMKII (Promega Corporation, Madison, WI) 1:200 in blocking solution, 60 hours at 4ºC; PBS, 6×10 min; swine anti-rabbit antibody (DakoCytomation, Solna, Sweden) 1:30 in blocking solution, 1 h; PBS, 3×10 min; rabbit peroxidase-antiperoxidase (DakoCytomation) in PBS with 0.5% bovine serum albumin, 1 h; PBS, 3×10 min; Tris-buffer (10 mM, pH 7.4) containing 0.9% NaCl (TBS), 10 min; 3,3´-diaminobenzidine in TBS, 10 min. Tissue sections were either mounted for light microscopy or osmicated and embedded in Durcupan ACM (Electron Microscopy Sciences) as described (Larsson *et al.*, 2001). Serial ultrathin sections of trimmed Durcupan embedded tissue were placed on Pioloform-coated nickel grids and

counterstained with uranyl acetate and lead citrate before examination in the electron microscope.

*Immunofluorescent labeling*

Immunofluorescent staining was carried out essentially as the immunoperoxidase staining up to the secondary antibody step, except that the ethanol steps were omitted and 0.1% Triton X-100 included in antibody and blocking solutions. For secondary detection, Alexa Fluor 594 donkey anti-rabbit IgG (Molecular Probes) was used at a 1:1000 concentration in blocking solution. Sections from rats subject to different perfusion protocols were processed together. After mounting, sections were examined blind to perfusion conditions using epifluorescence microscopy.

*Western blot analysis*

After decapitation, spinal cord tissue was excised from laminectomized spinal column, quickly frozen and pulverized in liquid $N_2$, and put on ice for 15 min in Tris-HCl buffer (pH 6.8) containing 2% SDS, 10% glycerol, a mixture of protease inhibitors (1:100; Sigma) and 1 mM each of NaF, $Na_3VO_4$ and PMSF. After sonication for 10 s, centrifugation at 2,000×g at 4ºC for 5 min, boiling for 3 min and centrifugation at 16,000×g at 4ºC for 15 min, the supernatant was subject to SDS-PAGE and transfer to a nitrocellulose membrane. The membrane was incubated in anti-pCaMKII (1:1000), followed by biotinylated swine anti-rabbit antibody (DakoCytomation) and Vectastain ABC solution (Vector Laboratories, Burlingame, CA). Immunoreactivity was detected by Western Lightning chemiluminescence kit (PerkinElmer).

*Tetrodotoxin (TTX) treatment of spinal cord slices*

The lumbosacral part of the spinal column was rapidly removed following decapitation and placed on ice in oxygenated (95% $O_2$, 5% $CO_2$) artificial cerebrospinal fluid (ACSF) containing (in mM): 124 NaCl, 26 $NaHCO_3$, 3 KCl, 1.3 $MgSO_4$, 2.5 $NaH_2PO_4$, 2.5 $CaCl_2$, and 20 glucose. Following excision from the vertebrae, spinal cord tissue was embedded in 2% agarose in ACSF and cut in 500 μm slices in ice-cold, oxygenated ACSF on a Vibratome, after which they were incubated for 3 h in oxygenated ACSF at 37ºC. Slices were incubated for 30–60 s in PBS at room temperature, prior to immersion fixation in 4% paraformaldehyde and 0.1% glutaraldehyde in PBS for 4 h at room temperature. For one set of slices, both the initial PBS buffer and the immersion fixative contained 1 μM TTX (Sigma), whereas another set of slices were incubated in parallel without TTX. After fixation, 40 μm sections were cut from the tissue slices on a freezing microtome and processed for immunofluorescent staining, as above.

*Postembedding immunogold labeling*

Postembedding immunogold labeling of pCaMKII was performed at room temperature. Ultrathin dorsal horn sections were etched for 1–2 s in a saturated solution of NaOH in ethanol, after which the sections were placed sequentially in: 50 mM glycine in Tris-buffer containing 0.3% NaCl and 0.1% Triton X-100 (TBST, pH 7.4), 10 min; 2% human serum albumin in TBST (TBST-HSA), 10 min; anti-pCaMKII 1:200–400 in TBST-HSA, 2 h; TBST, 2×10 min; TBST-HSA, 10 min; goat anti-rabbit antibody conjugated to 10 nm colloidal gold (Amersham Biosciences, Uppsala, Sweden) 1:20 in TBST-HSA, 1 h; distilled water, 10 min. After drying, the sections were counterstained with uranyl acetate and lead citrate. Double immunogold

labeling of SP and CGRP in adjacent sections was performed as above, but with primary antibody solution containing rat anti-SP (Chemicon) 1:200 and rabbit anti-CGRP (Bachem AG, Bubendorf, Germany) 1:400, and secondary antibody solution containing goat anti-rat antibody conjugated to 5 nm gold (British Biocell, Cardiff, UK; 1:40) and goat anti-rabbit antibody conjugated to 15 nm gold (Amersham Biosciences, Uppsala, Sweden; 1:20). The sections were examined in a JEOL electron microscope at 80kV and electron micrographs were obtained using a Gatan 791 MultiScan CCD camera.

The specificity of the anti-pCaMKII antibody towards the α and β isoforms of CaMKII autophosphorylated at $Thr^{286}$ (α) or $Thr^{287}$ (β) has been assessed by the manufacturer by western blot and immunofluorescence; the antibody also recognizes CaMKIIγ and/or CaMKIIδ (likely both) phosphorylated at $Thr^{287}$ (Lorenz et al., 2002). Immunocytochemistry using the antibody yields much reduced immunolabeling of visual cortex in a transgenic mouse expressing a mutant T286A CaMKIIα (residual labeling likely being indicative of other CaMKII isoforms phosphorylated at $Thr^{287}$), further supporting the specificity of the antibody towards the phosphorylated epitope (Taha et al., 2002). In a recent study, preembedding immunogold labeling using this antibody was shown to be elevated in postsynaptic densities of cultured hippocampal neurons following NMDA stimulation (Dosemeci et al., 2002). When anti-pCaMKII antibody was omitted from the primary antibody solution during the postembedding immunolabeling protocol, virtually no labeling, and specifically none associated with synapses, was observed.

*Quantitative analysis of postembedding immunolabeled sections*

Quantitative measurements were obtained in single pCaMKII postembedding immunogold labeled ultrathin dorsal horn sections from three rats. In an additional experiment, three serial sections from one rat, placed on a single grid, were immunolabeled and used for quantitative analysis. Average tissue labeling of pCaMKII-LI was estimated by measuring labeling densities in micrographs acquired at 25,000× of random regions of laminae I–II. All measurements of synapses were made on electron micrographs acquired at 80,000×, yielding a final image scale of 0.62 pixels/nm. Only those synapses were analyzed which demonstrated 1) a visible postsynaptic membrane, or a PSD distinctly separated from the synaptic cleft, along the entire synaptic length, and 2) presynaptic membrane visible along some part of the synapse. Only rarely did we observe putative perforated synapses in the pCaMKII labeled section, as judged by the presence of distinctly (but by less than 500 nm) separated PSDs involving the same pre- and postsynaptic profiles (4–5% of the total number of primary afferent synapses in a single section, as determined in Rat 3). The PSDs of such synapses were considered to be part of separate synapses; this affected the proportion of immunopositive synapses very marginally (determined in Rat 3). ImageJ v1.29–33 (http://rsb.info.nih.gov/ij/) and a plugin written for the purpose were used for manual image analysis of synaptic profiles. Micrographs were magnified to 200% during this step, so that each pixel was clearly visible on the screen. For each synaptic profile, outlines were made of the extracellular faces of the pre- and postsynaptic plasma membranes and of the cytoplasmic face of the PSD [a modification of the procedure used by Dosemeci et al. (2001)], the locations of the center of gold particles in the pre- and postsynaptic compartments were recorded, and the different sets of coordinates were submitted to a program implemented in Python

2.3 (http://www.python.org) for geometrical computations. Subsequent analysis of the resulting data was performed in GraphPad Prism v4 (GraphPad Software, San Diego, CA). Where applicable, values are expressed as mean ± SD.

When analyzing single immunolabeled sections, a gold particle was considered associated with the PSD if the center of the gold particle was lying directly over the PSD or within 25 nm of the outline of the PSD. Postsynaptic membrane length was defined as the length of postsynaptic plasma membrane between the two intercepts of the cytoplasmic face of the PSD with the plasma membrane, and PSD thickness was defined as the cross-sectional area of the PSD divided by postsynaptic membrane length (Dosemeci et al., 2001). When analyzing synaptic immunolabeling in serial sections, only the postsynaptic membrane was outlined; here, gold particles less than 75 nm from the PSD on the postsynaptic side or 25 nm on the presynaptic side were considered to be associated with the PSD.

To assess the association of immunogold label with dense core vesicles in peptidergic terminals, the distance of each presynaptic gold particle to the nearest discernible dense core vesicle was recorded using ImageJ. Gold particles farther than 200 nm from a dense core vesicle were discarded. For comparison, the distances of random points to the nearest dense core vesicles were also recorded. Similar strategies have previously been used to demonstrate the localization of amino acids (Gundersen et al., 2004) and vesicular glutamate transporters (Bezzi et al., 2004) to vesicular structures. We also determined the size distribution of dense core vesicles in the examined terminal population in an adjacent non-immunolabeled section by measurements of the long and short radii of the vesicles.

*Synaptic populations examined*

Three populations of primary afferent synapse were quantitatively analyzed with respect to pCaMKII-LI content. Nerve terminals in lamina I and outer lamina II with dense-core vesicles containing substance P (SP) and calcitonin gene-related peptide (CGRP) presumably originate from nociceptive primary afferent C and Aδ fibers (Lawson *et al.*, 1997; Hunt & Mantyh, 2001) and form synaptic contacts mainly with dorsal horn neurons possessing the neurokinin-1 receptor (Naim et al., 1997; McLeod et al., 1998; Todd et al., 2002). Dense sinusoid axon terminals (DSAs), sinuously shaped terminals with dark axoplasm and tightly packed clear vesicles of non-uniform size, are the central endings of another, mainly non-peptidergic, population of C fiber nociceptor (Ralston & Ralston, 1979; Knyihar-Csillik *et al.*, 1982; Ribeiro-da-Silva & Coimbra, 1982), which bind isolectin B4 (Alvarez *et al.*, 2004; Gerke & Plenderleith, 2004) and express the $P2X_3$ receptor (Vulchanova et al., 1998). This fiber population terminates preferentially in inner lamina II (IIi). Both peptidergic and non-peptidergic nociceptors often express the capsaicin receptor, TRPV1 (Tominaga et al., 1998; Guo et al., 1999; Guo et al., 2001), and are activated by similar noxious stimuli (Hunt & Mantyh, 2001), although they differ somewhat in their heat responses and electrophysiological characteristics (Stucky & Lewin, 1999). Central terminals of presumed low-threshold mechanosensitive primary afferent fiber (LTMs) in laminae IIi–IV were identified by their glomerular arrangement, electron-lucid axoplasm and clear, uniformly sized synaptic vesicles (Maxwell & Réthelyi, 1987). These terminals showed morphological characteristics identical to those of terminals labelled by cholera toxin B-horseradish peroxidase, as observed in previous studies (Broman et al., 1993; Larsson et al., 2001). The location of all sampled terminals was marked on low-power electron micrographs of the sections.

Synapses formed by SP/CGRP-containing primary afferent terminals (SP/CGRP synapses) were identified by screening an adjacent ultrathin section which had been immunogold labeled against SP and CGRP, while synapses formed by DSAs (DSA synapses) and LTMs (LTM synapses) were morphologically identified in a second adjacent section, which had not been subject to any immunolabeling. Thus, quantitative analysis of pCaMKII labeling of the different types of synapse were made in the same section in each rat, allowing direct comparison of the immunolabeling between the synaptic populations. Apart from allowing selection of synapses based on identification of the presynaptic component, this procedure also enabled unbiased selection with respect to pCaMKII-LI.

## Results

*General observations*

In the light microscope, spinal cord sections immunoperoxidase labeled for pCaMKII exhibited pCaMKII-like immunoreactivity (pCaMKII-LI) throughout the gray matter. Immunolabeled cell bodies were observed in all laminae; for instance, in the ventral horn many motoneurons were labeled (not shown). However, the superficial dorsal horn exhibited the most prominent immunolabeling; here, both neuropil and cell bodies showed dense immunoreactivity (Fig. 1A). pCaMKII-LI was also present, although fainter than in laminae I–II, in neuropil and somata in the deep dorsal horn (Fig. 1A). By western blot analysis of whole rat spinal cord homogenate we observed an immunoreactive band of ~55 kDa (not shown), thus corroborating the ability of the antibody to detect pCaMKII in naïve spinal cord (see also Galan *et al.*, 2004).

Electron microscopic examination of immunoperoxidase labeled laminae I–III revealed numerous asymmetric synapses exhibiting reaction product in their postsynaptic density. Specifically, many synapses formed by central terminals of glomeruli displayed unequivocal immunolabeling. Many of these glomerular terminals could be identified as DSAs, of presumed non-peptidergic C fiber origin (Fig. 1B), whereas other terminals at the center of glomeruli and forming immunopositive synapses were identified as LTMs, i.e., terminals of presumed low-threshold mechanosensitive primary afferent fibers (Fig. 1C). In addition to the synaptic immunolabeling, we observed strong cytosolic immunoreactivity in many dendritic structures, particularly in laminae I–II (Fig. 1B) and neuronal cell bodies; in presynaptic terminals, immunolabeling was only evident in the vicinity of the presynaptic plasma membrane.

In ultrathin dorsal horn sections processed for postembedding pCaMKII immunogold labeling, gold particles were present over most tissue components throughout the dorsal horn, although at low densities in most structures. The average tissue density of immunolabeling in laminae I–II ranged between 3.4 and 6.6 gold particles/$\mu m^2$ in the different sections (Table 1). Note that this estimate not only reflects possible unspecific background labeling, because strongly immunopositive structures such as synapses (see below) were included, and a substantial basal level of cytosolic pCaMKII is present in the dorsal horn (Fang et al., 2002). Thus, a proportion of the cytosolic pCaMKII-LI observed in our preparations likely indicated actual pCaMKII. Some pCaMKII-LI was associated with cell bodies and dendrites; however, the most prominent immunogold labeling was associated with asymmetric (presumably excitatory) synaptic specializations, in agreement with our observations from preembedding immunolabeled dorsal horn.

*Is pCaMKII upregulated during perfusion fixation?*

Brief ischemia during perfusion of animals could possibly, via increased dendritic or axonal $Ca^{2+}$ levels, lead to phosphorylation of PSD-associated and cytosolic CaMKII. However, extending the rinsing time prior to fixative administration from 30 s to 90 s did not result in increased levels of pCaMKII in the dorsal horn (Fig. 2A), which suggests either that on these short time scales, pCaMKII is not sensitive to ischemic conditions, or that an ischemia-induced saturation of pCaMKII levels occurs very rapidly. The latter possibility appears unlikely considering the results of the lidocaine experiments (see below).

During fixation of nervous tissue with aldehydes, neuronal activity triggered by these substances could conceivably lead to rapid phosphorylation of synaptic or

extrasynaptic CaMKII. To investigate this possibility, we incubated spinal cord slices with or without TTX immediately prior to and during immersion fixation in aldehydes. The level of pCaMKII immunofluorescence in TTX treated spinal cord slices was not appreciably different from that observed in slices fixed without TTX (Fig 2B). However, the adverse impact of the slicing procedure on the integrity of the tissue may have masked a possible effect of aldehyde fixation on the level of pCaMKII. To address this concern, we performed immunofluorescent staining of pCaMKII on spinal cord sections from perfusion-fixed animals which were rinsed transcardially with PBS containing 3 mM lidocaine prior to the administration of fixative. The lidocaine concentration used was threefold higher than that sufficient to completely inhibit voltage-gated $Na^+$ channels (Gold *et al.*, 1998) and abolish compound action potentials (Nagy & Woolf, 1996) in primary afferent neurons, while lower than the concentration shown to elevate intracellular $Ca^{2+}$ in these neurons (Gold *et al.*, 1998). Thus, although it is difficult to estimate the local tissue concentration of systemically administered lidocaine, the local concentrations attained here were likely enough to substantially inhibit aldehyde-induced neuronal excitation. The presence of lidocaine in the rinsing buffer considerably diminished or abolished the strong muscle contractions normally observed at the onset of fixative perfusion, indicating that the lidocaine dose was indeed effective. Immunofluorescent pCaMKII staining of spinal cord sections from rats rinsed with lidocaine-containing buffer was not weaker than the staining obtained in sections from rats perfused with PBS prior to fixation. On the contrary, in three of four lidocaine-subjected rats, pCaMKII-LI were instead substantially increased compared to normally perfused rats (Fig. 2C); among these, pCaMKII staining was most intense in the one rat where muscle contractions were completely abolished during fixation. This finding is difficult to explain in the

present context, as the lidocaine concentration used reportedly does not enhance primary afferent neuronal $Ca^{2+}$ levels (Gold *et al.*, 1998). Nevertheless, the observation confirms that the immunoreactivity reflects a tissue component which may be rapidly regulated, as would be expected if the antibody specifically recognizes a phosphoprotein.

Taken together, these observations suggest that the pCaMKII immunolabeling presently detected in naïve rat dorsal horn by postembedding immunogold and other techniques represents submaximal pCaMKII levels which are not substantially affected either by ischemic or aldehyde-induced neuronal excitation during perfusion fixation.

*Quantitative analysis of pCaMKII-LI in primary afferent synapses*

We used postembedding immunogold labeled tissue sections for quantitative analysis of the ultrastructural localization of pCaMKII-LI in the dorsal horn of naïve rats. Most synapses formed by SP/CGRP terminals, which originate from peptidergic, presumed nociceptive primary afferent fibers, were found in lamina I and outer lamina II, whereas DSA synapses formed by nonpeptidergic C fibers were predominantly located in lamina IIi. LTM synapses were sampled from laminae IIi–IV (most of them were found in lamina III). All synaptic populations were sampled from the complete mediolateral extent of the dorsal horn. pCaMKII immunolabeled DSA synapses (Fig. 3), SP/CGRP synapses (Fig. 4) and LTM synapses (Fig. 5) were numerous. Gold particles were clearly enriched over PSDs in all examined synaptic populations, average immunolabeling densities within PSDs being up to ~25 times higher than the average tissue immunolabeling (Table 1). The enrichment of pCaMKII-LI over PSDs relative to the overall tissue labeling was higher in Rat 3 as compared to the other two

rats, which may indicate that a higher signal-to-noise ratio was obtained in this experiment. Postsynaptic dendrites with immunolabeled PSDs sometimes contained synaptic-like vesicles, thus likely originating from inhibitory local circuit neurons (Todd, 1996).

In the following, except where noted, we considered gold particles centered within 25 nm of the PSD as associated with the PSD, as the estimated spatial resolution of the immunogold labeling when using 10 nm gold is ~25 nm (Ottersen, 1989). Because immunolabeling was considerably enriched over PSDs as compared to the average tissue labeling, and because a sizeable proportion of the observed cytosolic labeling is also likely to be specific (see above), PSDs associated with one or more gold particles were considered immunopositive. We estimate, based on mean PSD dimensions in the various synaptic samples, that if the immunolabeling was randomly scattered over the tissue, on average 0.14 ± 0.05 gold particles would be associated with each synapse (i.e., within 25 nm of the PSD). Therefore, the proportions of synapses with specific label may be slightly overestimated. However, when we set the threshold of immunopositivity to two gold particles, the differences in proportion of labeled PSDs between different synapse types remained similar and statistically significant (see below). Because a threshold of two gold particles would instead considerably underestimate the number of specifically labeled synapses, we chose to use the lower threshold throughout this study.

In single immunolabeled sections, immunopositive PSDs among DSA synapses were more frequent than among SP/CGRP synapses in all rats, although only slightly so in Rat 3. However, LTM synapses were significantly less frequently immunolabeled than either DSA or SP/CGRP synapses (Table 1). The frequency distributions of PSD immunoreactivity were similar among DSA and SP/CGRP

synapses, most PSDs containing relatively few gold particles but some exhibiting stronger immunoreactivity (Fig. 6). LTM synapses also showed a similar distribution of PSD immunoreactivity, except for a larger proportion of immunonegative PSDs (Fig. 6).

The summed linear density of pCaMKII-LI (total number of gold particles associated with PSDs divided by the summed postsynaptic membrane length) was consistently higher in DSA synapses than in SP/CGRP and LTM synapses and in SP/CGRP synapses compared to LTM synapses (Table 2), although the only significant difference was that between DSA and LTM synapses ($P < 0.05$, repeated measures ANOVA followed by Tukey's post hoc test). However, when excluding immunonegative synapses, linear densities of pCaMKII-LI were relatively similar between synaptic populations (Table 2). No differences were detected between synapses in the medial and lateral halfs of the dorsal horn (Mann-Whitney U test, $P > 0.05$; data not shown).

*Synaptic pCaMKII-LI in serial sections*

Due to the limited sensitivity of the immunogold labeling, a larger proportion of immunonegative LTM synapses compared to nociceptive primary afferent synapses in a single section may reflect either that a larger subpopulation of LTM synapses lack pCaMKII altogether, or that LTM synapses generally contain lower levels of pCaMKII. In order to establish a more reliable estimate of the fraction of primary afferent synapses containing PSD-associated pCaMKII, we traced DSA and LTM synapses ($n = 24$ in each sample) through three consecutive pCaMKII immunolabeled sections from Rat 3. Here, synapses were considered immunopositive if at least one gold particle was less than 75 nm on the postsynaptic side or 25 nm on the presynaptic

side from the postsynaptic plasma membrane. Although 29% of DSA synapses were immunonegative in the first section, only one synapse (4%) lacked immunoreactivity in both sections 1 and 2; this synapse was immunonegative also in the third section (Fig. 7A). Of LTM synapses, 38% were immunonegative in section 1, whereas 21% were immunonegative both in sections 1 and 2. Two LTM synapses (8%) did not display gold particles in any of the three sections (Fig. 7A). For each synapse we also determined the summed linear density, i.e., the total number of postsynaptic gold particles in the three sections per μm of summed synaptic length in the sections. DSA synapses contained 5.8 ± 3.6 gold particles/μm, whereas LTM synapses contained 3.0 ± 1.9 gold particles/μm (Fig. 7B); this difference was statistically significant ($P = 0.002$, Student's $t$ test, two-tailed). Thus, analysis of serial immunolabeled sections indicated that all or nearly all synapses in the examined populations contained pCaMKII, but that pCaMKII levels were on average nearly twice as high in DSA synapses as in LTM synapses.

*Subsynaptic distribution of pCaMKII-LI*

The distributions of gold particles along the axodendritic axis of the synapse for the examined synaptic populations are shown in Fig. 8. Strong immunolabeling was evident below the postsynaptic plasma membrane, with a broad postsynaptic peak up to 60 nm below the postsynaptic membrane, and sharp declines in immunolabeling in the synaptic cleft (0–20 nm outside the postsynaptic membrane) and at distances from the postsynaptic membrane greater than ~60 nm. As the PSD thickness of immunopositive synapses (i.e., with gold particles within their PSD) was 41 ± 13 nm, 44 ± 11 nm and 40 ± 11 nm for DSA, SP/CGRP and LTM synapses, respectively, these gold particle distributions supported preferential localization of pCaMKII-LI

within the boundaries of the PSD. Mean distance to the postsynaptic membrane of gold particles located immediately over the PSD was 27 ± 16 nm for DSA synapses, 27 ± 14 nm for SP/CGRP synapses and 23 ± 14 nm for LTM synapses. The axodendritic localization of immunolabeling thus corresponded well with a spatially restricted localization of pCaMKII throughout the thickness of the PSD, possibly except for the region immediately (~10 nm) below the postsynaptic plasma membrane, a region within which relative lack of antigen was consistent with our data. In accordance with our observation of pCaMKII-LI throughout the extent of the PSD in the axodendritic axis, there was in most (7 of 9) synaptic samples a significant positive correlation (Spearman; $P < 0.05$) between the linear density of pCaMKII-LI (i.e., the number of gold particles associated with the PSD per unit length of synaptic membrane) and PSD thickness. No significant positive correlation was observed between the linear density of pCaMKII-LI and the length of the postsynaptic membrane.

In order to investigate the mediolateral (tangential) distribution of postsynaptic pCaMKII-LI, normalized mediolateral positions of gold particles within 25 nm of PSDs with a postsynaptic membrane length of more than 200 nm (171 of 599 synapses were excluded by this criterion) were binned. Data from all rats were pooled. In all examined synaptic populations, immunolabeling extended relatively evenly throughout the mediolateral axis of the PSD to the synaptic periphery, whereas a rapid decrease in immunolabeling was evident in the perisynaptic region (Fig. 9).

Although pCaMKII-LI was observed throughout PSDs both along the axodendritic and mediolateral axes, it could not be inferred from single immunolabeled sections whether pCaMKII was evenly distributed within individual PSDs. If this was the case, it would be expected that in serial immunolabeled sections,

the density of immunolabeling of a synapse in one section correlates with the labeling density of the synapse in the adjacent section. However, there was a large variability in immunogold label between consecutive sections through individual synapses; for example, one LTM synapse was immunonegative in two sections but exhibited 15.8 gold particles/μm in the third section. Indeed, we did not observe any correlations of linear densities of pCaMKII-LI in DSA or LTM synapses between the middle section and the two adjacent sections; Spearman *r* values were -0.18 and 0.38 for DSA synapses, and –0.11 and 0.05 for LTM synapses ($P > 0.05$ for all correlations), suggesting considerable heterogeneity in pCaMKII levels between sections through individual synapses.

*Presynaptic pCaMKII-LI*

The pattern of pCaMKII-LI in the axodendritic axis of primary afferent synapses also suggested the presence of presynaptic pCaMKII (Fig. 8). Gold particle density in the presynaptic region bounded by the lateral edges of the synapse and 10–100 nm from the postsynaptic membrane was 2.0 ± 0.7 times the average tissue labeling (Table 3); this enrichment was statistically significant ($P = 0.002$, one sample *t* test, two-tailed). No differences between the examined synaptic populations were evident with regards to the immunolabeling of presynaptic axoplasm near the synaptic membrane. However, in SP/CGRP terminals, gold particles were often found in association with dense core vesicles (DCVs; Fig. 10A). Quantitative analysis of pCaMKII-LI in SP/CGRP terminals revealed enrichment of gold particles at a distance of 20–60 nm from the center of the nearest DCV (Fig. 10B). This distribution was significantly different from the distribution of distances of randomly placed points to the nearest DCV center ($P < 0.0001$, $\chi^2$ test). Because dense core vesicles were found to have a

radius of 43 ± 8 nm, this pattern of pCaMKII-LI was in agreement with a localization of pCaMKII in proximity to the membrane of DCVs.

## Discussion

We have shown, using pre- and postembedding immunolabeling methods, that many excitatory synapses in laminae I–IV of the rat dorsal horn contain considerable pCaMKII-like immunoreactivity at their PSD. Quantitative analysis of postembedding immunolabeled tissue indicated that while the majority of primary afferent synapses exhibited immunopositive PSDs, those PSDs associated with presumed nociceptive primary afferent fiber terminals contained substantially higher levels of immunolabeling than those postsynaptic to presumed low-threshold mechanosensitive primary afferent fibers.

### *Methodological considerations*

Our results suggest that the brief ischemia inevitably occurring during perfusion of animals did not lead to enhanced phosphorylation of CaMKII, likely to a large extent due to the short interval between chest opening and the onset of tissue fixation. Moreover, the absence of $Ca^{2+}$ in the rinsing buffer presumably limited the $Ca^{2+}$ current that may arise through activated NMDA receptors in ischemia. In support of this, in adult hippocampal slices, intracellular $Ca^{2+}$ levels in the neuropil do not increase during the first three minutes of ischemia (Zhang & Lipton, 1999), and release of $Ca^{2+}$ from internal stores is small during the early phase of ischemia (Zhang & Lipton, 1999). We therefore estimate that any ischemia-induced effect on CaMKII phosphorylation in our preparations is marginal. Moreover, pCaMKII levels in the spinal cord did not appear to be enhanced by neuronal activity during aldehyde fixation.

The postembedding immunogold labeling procedure yields, with some antibodies, unspecific labeling of protein-rich domains, such as PSDs or dense core vesicles

(Nagy *et al.*, 2003); it is also conceivable that the phosphospecificity of the pCaMKII antibody used here may be compromised under the postembedding labeling conditions. However, the former possibility is not supported by the differential PSD labeling of different types of synapse observed in this study, or by the apparent membrane-associated labeling of dense core vesicles. Furthermore, work of other investigators corroborates the applicability of the antibody for labeling of synaptic and phosphorylated CaMKII in preembedding and light microscopy immunocytochemistry (Dosemeci et al., 2002; Taha et al., 2002; Rodrigues et al., 2004), and the similarities observed here in the pattern of primary afferent synaptic immunoreactivity between pre- and postembedding immunolabeled tissue supports the specificity of the antibody also in postembedding immunolabeling.

It should be noted that the phosphospecific antibody used in the present study recognizes not only CaMKIIα but also the CaMKIIβ isoform, and likely the γ and δ isoforms as well (Lorenz et al., 2002). CaMKIIα is primarily expressed in the superficial dorsal horn whereas CaMKIIβ shows a more even distribution throughout the spinal cord gray matter (Terashima et al., 1994). Thus, it is likely that some of the observed pCaMKII-LI can be attributed to phosphorylated isoforms other than CaMKIIα. Further, the different expression patterns of CaMKII isoforms between laminae imply that the proportions of isoforms at the PSD may differ considerably between primary afferent synapses. By the methodology used in the present study it would therefore be difficult to estimate the ratio of phosphorylated versus non-phosphorylated CaMKII subunits at different synapses, as it would require the use of a combination of antibodies detecting, with known labeling efficiencies, the different CaMKII isoforms.

*Synaptic organization of pCaMKII*

The observed distribution of pCaMKII-LI along the axodendritic axis of the synapse supports a localization of pCaMKII primarily within the PSD. Immunogold labeling within the PSD appeared to extend at high density to the cytosolic edge of the PSD, with a mean distance to the postsynaptic membrane of ~25 nm, but was sparser in the domain immediately below (~10 nm) the postsynaptic plasma membrane. This axodendritic organization of pCaMKII immunolabeling within the PSD is consistent with the distribution of native CaMKII reported from isolated forebrain PSDs (Petersen et al., 2003). The large variability in pCaMKII-LI between consecutive sections through a single synapse may be at least partly explained by an uneven distribution of CaMKII itself between subdomains of the PSD (Petersen et al., 2003).

*Functional significance of pCaMKII within the PSD of primary afferent synapses*

Whereas the involvement of CaMKII in the induction of NMDA receptor-dependent LTP is firmly established, the situation is less clear with regards to its role in the maintenance of LTP. Theoretical work suggest that CaMKII together with protein phosphatase 1 (PP1) may constitute a bistable switch in the postsynaptic density, where the CaMKII is either highly or weakly phosphorylated at $Thr^{286/287}$ (Zhabotinsky, 2000; Lisman & Zhabotinsky, 2001). Although we could not estimate the proportion of CaMKII subunits phosphorylated at $Thr^{286/287}$ (see above), our observations indicate that significant amounts of pCaMKII is present at all or nearly all primary afferent synapses, suggesting that most such synapses contain CaMKII in a highly phosphorylated state. Given the ability of CaMKII to modify synaptic strength, e.g. by phosphorylation and recruitment of AMPA receptors (Barria et al., 1997; Derkach et al., 1999; Hayashi et al., 2000; Lee et al., 2000; Poncer et al., 2002),

it appears likely that the abundant PSD-associated pCaMKII presently demonstrated in primary afferent synapses indeed affects the strength of these synapses. Interestingly, recent evidence suggest that following hippocampal LTP induction, autophosphorylation of CaMKII may outlast a transient increase in autonomous CaMKII activity, possibly reflecting a role, dissociated from its kinase activity, for the autophosphorylated enzyme in LTP maintenance (Lengyel *et al.*, 2004).

Even if persistence of pCaMKII within the PSD can be explained by bistability of the CaMKII–PP1 system, the mechanisms underlying induction of CaMKII phosphorylation at primary afferent synapses remain to be clarified. This issue is particularly intriguing in the case of synapses of nociceptive fibers, which in the absence of noxious stimuli show little ongoing discharge (Campbell & Meyer, 1996). Their low, unperceived activity may be sufficient to induce postsynaptic autophosphorylation of CaMKII, e.g., at postsynaptic membranes expressing $Ca^{2+}$-permeable AMPA receptors (Gu et al., 1996). However, because such AMPA receptors are sparse in lamina IIi (Engelman et al., 1999), other mechanisms, e.g., such that are dependent on heterosynaptic input, are likely to be involved.

Regardless, the present findings suggest that nociceptive synapses could be depotentiated for the purpose of reducing pain. Indeed, depotentiation or long-term depression of high-threshold primary afferent synaptic transmission has been demonstrated (Sandkühler et al., 1997; Liu et al., 1998). Such weakening of nociceptive primary afferent synapses may underly the prolonged analgesia observed after cutaneous low-frequency stimulation of thin-caliber primary afferents (Nilsson & Schouenborg, 1999).

*pCaMKII at low threshold vs nociceptive primary afferent synapses*

Synapses formed by the central endings of low-threshold mechanosensitive primary afferent fibers appeared to contain less pCaMKII within their PSD than did synapses formed by terminals originating from non-peptidergic (and likely also peptidergic) nociceptive primary afferent fibers, suggesting differential regulation of basal pCaMKII at these synapses. Specifically, the higher levels of pCaMKII immunolabeling at synapses of nociceptive primary afferent fibers compared to those of low-threshold primary afferent fibers indicate that autophosphorylation of CaMKII is not a simple function of presynaptic activity.

High-threshold C fiber responses readily undergo LTP (Sandkühler, 2000; Willis, 2002; Ji et al., 2003), whereas low-threshold Aβ fiber synaptic transmission is less susceptible to LTP induction (Svendsen et al., 1998; Svendsen et al., 1999). The higher levels of pCaMKII in PSDs of nociceptive primary afferent synapses as compared to PSDs of LTM synapses could tentatively contribute to this difference: If CaMKII is translocated to the postsynaptic density following strong synaptic activity, it may easily be autophosphorylated if the concentration of autophosphorylated CaMKII subunits is already high, and thus PP1 saturated, in the postsynaptic density. Conversely, only a slight, transient phosphorylation of translocated CaMKII molecules conceivably occurs in postsynaptic densities with unsaturated PP1 due to low levels of pCaMKII (Lisman & Zhabotinsky, 2001). Indeed, phosphatase inhibitors prolong association of CaMKII with postsynaptic sites (Shen et al., 2000; Dosemeci et al., 2002).

*Presynaptic pCaMKII in primary afferent terminals*

Significant pCaMKII postembedding immunogold labeling was observed over the presynaptic compartment in all examined synaptic populations; moreover, in

SP/CGRP terminals we found immunolabeling associated with dense core vesicles. Several presynaptic molecular targets of CaMKII have been identified (Colbran, 2004). For example, vesicle-associated CaMKII may inhibit the association of synapsin I to small synaptic vesicles, thus mobilizing such vesicles to the readily releasable pool (Greengard et al., 1993); CaMKII has also been implicated in the regulation of dense core vesicle exocytosis (Schweitzer *et al.*, 1995; Wang *et al.*, 2002).

*Conclusions*

The present observations suggest that a certain level of pCaMKII is common within PSDs of central glutamatergic synapses *in vivo*. Specifically, high levels of pCaMKII **immunoreactivity were** present postsynaptically at nociceptive primary afferent synapses in naïve rats (i.e., rats not subject to experimental noxious stimulation), whereas at presumed low-threshold primary afferent synapses, pCaMKII **immunolabeling was** also present but at considerably lower levels. Thus, PSD-associated pCaMKII appears to be available at most synapses to contribute to maintenance and plasticity of synaptic strength. Additionally, selective weakening of nociceptive synapses by dephosphorylation of synaptic CaMKII (by pharmacological or other means) could conceivably be used as a route to pain inhibition.

*Acknowledgements*

This work was supported by the Swedish Research Council (project no. 14276), the Royal Physiographic Society, the Crafoord Foundation and the Thorsten and Elsa Segerfalk Foundation.

*Abbreviations*

ACSF, artificial cerebrospinal fluid; CaMKII, $Ca^{2+}$/calmodulin-dependent protein kinase II; CGRP, calcitonin gene-related peptide; DCV, dense core vesicle; DSA, dense sinusoid axon terminal; LTM, low-threshold mechanosensitive primary afferent terminal; pCaMKII, CaMKII phosphorylated at $Thr^{286/287}$; pCaMKII-LI, pCaMKII-like immunoreactivity; PP1, protein phosphatase 1; PBS, phosphate-buffered saline; PSD, postsynaptic density; SP, substance P; TBS, Tris-buffered saline; TBST, TBS with Triton X-100; TBST-HSA, TBST with human serum albumin; TTX, tetrodotoxin

## References


Alvarez, F.J., Villalba, R.M., Zerda, R. & Schneider, S.P. (2004) Vesicular glutamate transporters in the spinal cord, with special reference to sensory primary afferent synapses. *J Comp Neurol*, **472**, 257-280.

Barria, A., Muller, D., Derkach, V., Griffith, L.C. & Soderling, T.R. (1997) Regulatory phosphorylation of AMPA-type glutamate receptors by CaM-KII during long-term potentiation. *Science*, **276**, 2042-2045.

Bezzi, P., Gundersen, V., Galbete, J.L., Seifert, G., Steinhauser, C., Pilati, E. & Volterra, A. (2004) Astrocytes contain a vesicular compartment that is competent for regulated exocytosis of glutamate. *Nat Neurosci*, **7**, 613-620.

Broman, J., Anderson, S. & Ottersen, O.P. (1993) Enrichment of glutamate-like immunoreactivity in primary afferent terminals throughout the spinal cord dorsal horn. *Eur J Neurosci*, **5**, 1050-1061.

Campbell, J.N. & Meyer, R.A. (1996) Cutaneous nociceptors. In Belmonte, C., Cervero, F. (eds.) *Neurobiology of nociceptors*. Oxford UP, Oxford, pp. 117-145.

Carlton, S.M. & Hayes, E.S. (1989) Dynorphin A(1-8) immunoreactive cell bodies, dendrites and terminals are postsynaptic to calcitonin gene-related peptide primary afferent terminals in the monkey dorsal horn. *Brain Res*, **504**, 124-128.

Colbran, R.J. (2004) Targeting of calcium/calmodulin-dependent protein kinase II. *Biochem J*, **378**, 1-16.

Derkach, V., Barria, A. & Soderling, T.R. (1999) $Ca^{2+}$/calmodulin-kinase II enhances channel conductance of α-amino-3-hydroxy-5-methyl-4-isoxazolepropionate type glutamate receptors. *Proc Natl Acad Sci U S A*, **96**, 3269-3274.

Dosemeci, A., Tao-Cheng, J.H., Vinade, L., Winters, C.A., Pozzo-Miller, L. & Reese, T.S. (2001) Glutamate-induced transient modification of the postsynaptic density. *Proc Natl Acad Sci U S A*, **98**, 10428-10432.

Dosemeci, A., Vinade, L., Winters, C.A., Reese, T.S. & Tao-Cheng, J.H. (2002) Inhibition of phosphatase activity prolongs NMDA-induced modification of the postsynaptic density. *J Neurocytol*, **31**, 605-612.

Engelman, H.S., Allen, T.B. & MacDermott, A.B. (1999) The distribution of neurons expressing calcium-permeable AMPA receptors in the superficial laminae of the spinal cord dorsal horn. *J Neurosci*, **19**, 2081-2089.

Fang, L., Wu, J., Lin, Q. & Willis, W.D. (2002) Calcium-calmodulin-dependent protein kinase II contributes to spinal cord central sensitization. *J Neurosci*, **22**, 4196-4204.

Fukunaga, K., Muller, D. & Miyamoto, E. (1995) Increased phosphorylation of $Ca^{2+}$/calmodulin-dependent protein kinase II and its endogenous substrates in the induction of long term potentiation. *J. Biol. Chem.*, **270**, 6119-6124.

Galan, A., Laird, J.M. & Cervero, F. (2004) In vivo recruitment by painful stimuli of AMPA receptor subunits to the plasma membrane of spinal cord neurons. *Pain*, **112**, 315-323.

Garry, E.M., Moss, A., Delaney, A., O'Neill, F., Blakemore, J., Bowen, J., Husi, H., Mitchell, R., Grant, S.G. & Fleetwood-Walker, S.M. (2003) Neuropathic sensitization of behavioral reflexes and spinal NMDA receptor/CaM kinase II interactions are disrupted in PSD-95 mutant mice. *Curr Biol*, **13**, 321-328.

Gerke, M.B. & Plenderleith, M.B. (2004) Ultrastructural analysis of the central terminals of primary sensory neurones labelled by transganglionic transport of *bandeiraea simplicifolia* i-isolectin $B_4$. *Neuroscience*, **127**, 165-175.

Gleason, M.R., Higashijima, S., Dallman, J., Liu, K., Mandel, G. & Fetcho, J.R. (2003) Translocation of CaM kinase II to synaptic sites in vivo. *Nat Neurosci*, **6**, 217-218.

Gold, M.S., Reichling, D.B., Hampl, K.F., Drasner, K. & Levine, J.D. (1998) Lidocaine toxicity in primary afferent neurons from the rat. *J Pharmacol Exp Ther*, **285**, 413-421.

Greengard, P., Valtorta, F., Czernik, A.J. & Benfenati, F. (1993) Synaptic vesicle phosphoproteins and regulation of synaptic function. *Science*, **259**, 780-785.

Gu, J.G., Albuquerque, C., Lee, C.J. & MacDermott, A.B. (1996) Synaptic strengthening through activation of $Ca^{2+}$-permeable AMPA receptors. *Nature*, **381**, 793-796.

Gundersen, V., Holten, A.T. & Storm-Mathisen, J. (2004) GABAergic synapses in hippocampus exocytose aspartate on to NMDA receptors: quantitative immunogold evidence for co-transmission. *Mol Cell Neurosci*, **26**, 156-165.

Guo, A., Simone, D.A., Stone, L.S., Fairbanks, C.A., Wang, J. & Elde, R. (2001) Developmental shift of vanilloid receptor 1 (VR1) terminals into deeper regions of the superficial dorsal horn: correlation with a shift from TrkA to Ret expression by dorsal root ganglion neurons. *Eur J Neurosci*, **14**, 293-304.

Guo, A., Vulchanova, L., Wang, J., Li, X. & Elde, R. (1999) Immunocytochemical localization of the vanilloid receptor 1 (VR1): relationship to neuropeptides, the $P2X_3$ purinoceptor and IB4 binding sites. *Eur J Neurosci*, **11**, 946-958.

Hayashi, Y., Shi, S.H., Esteban, J.A., Piccini, A., Poncer, J.C. & Malinow, R. (2000) Driving AMPA receptors into synapses by LTP and CaMKII: requirement for GluR1 and PDZ domain interaction. *Science*, **287**, 2262-2267.

Hunt, S.P. & Mantyh, P.W. (2001) The molecular dynamics of pain control. *Nat Rev Neurosci*, **2**, 83-91.

Ikeda, H., Heinke, B., Ruscheweyh, R. & Sandkühler, J. (2003) Synaptic plasticity in spinal lamina I projection neurons that mediate hyperalgesia. *Science*, **299**, 1237-1240.

Ji, R.R., Kohno, T., Moore, K.A. & Woolf, C.J. (2003) Central sensitization and LTP: do pain and memory share similar mechanisms? *Trends Neurosci*, **26**, 696-705.

Knyihar-Csillik, E., Csillik, B. & Rakic, P. (1982) Ultrastructure of normal and degenerating glomerular terminals of dorsal root axons in the substantia gelatinosa of the rhesus monkey. *J Comp Neurol*, **210**, 357-375.

Larsson, M., Persson, S., Ottersen, O.P. & Broman, J. (2001) Quantitative analysis of immunogold labeling indicates low levels and non-vesicular localization of L-aspartate in rat primary afferent terminals. *J Comp Neurol*, **430**, 147-159.

Lawson, S.N., Crepps, B.A. & Perl, E.R. (1997) Relationship of substance P to afferent characteristics of dorsal root ganglion neurones in guinea-pig. *J Physiol*, **505 ( Pt 1)**, 177-191.

Lee, H.K., Barbarosie, M., Kameyama, K., Bear, M.F. & Huganir, R.L. (2000) Regulation of distinct AMPA receptor phosphorylation sites during bidirectional synaptic plasticity. *Nature*, **405**, 955-959.

Lengyel, I., Voss, K., Cammarota, M., Bradshaw, K., Brent, V., Murphy, K.P., Giese, K.P., Rostas, J.A. & Bliss, T.V. (2004) Autonomous activity of CaMKII is only transiently increased following the induction of long-term potentiation in the rat hippocampus. *Eur J Neurosci*, **20**, 3063-3072.

Lisman, J., Schulman, H. & Cline, H. (2002) The molecular basis of CaMKII function in synaptic and behavioural memory. *Nat Rev Neurosci*, **3**, 175-190.

Lisman, J.E. & Zhabotinsky, A.M. (2001) A model of synaptic memory: a CaMKII/PP1 switch that potentiates transmission by organizing an AMPA receptor anchoring assembly. *Neuron*, **31**, 191-201.

Liu, X.G., Morton, C.R., Azkue, J.J., Zimmermann, M. & Sandkühler, J. (1998) Long-term depression of C-fibre-evoked spinal field potentials by stimulation of primary afferent Aδ-fibres in the adult rat. *Eur J Neurosci*, **10**, 3069-3075.

Lorenz, J.M., Riddervold, M.H., Beckett, E.A., Baker, S.A. & Perrino, B.A. (2002) Differential autophosphorylation of CaM kinase II from phasic and tonic smooth muscle tissues. *Am J Physiol Cell Physiol*, **283**, C1399-1413.

Maxwell, D.J. & Réthelyi, M. (1987) Ultrastructure and synaptic connections of cutaneous afferent fibres in the spinal cord. *Trends Neurosci*, **10**, 117-123.

McLeod, A.L., Krause, J.E., Cuello, A.C. & Ribeiro-da-Silva, A. (1998) Preferential synaptic relationships between substance P-immunoreactive boutons and neurokinin 1 receptor sites in the rat spinal cord. *Proc Natl Acad Sci U S A*, **95**, 15775-15780.

Molander, C., Xu, Q. & Grant, G. (1984) The cytoarchitectonic organization of the spinal cord in the rat. I. The lower thoracic and lumbosacral cord. *J Comp Neurol*, **230**, 133-141.

Nagy, G.G., Maxwell, D.J., Watanabe, M., Mishina, M., Sakimura, K. & Todd, A.J. (2003) Apparent non-specific immunogold labelling with an NMDA receptor antibody. Program No. 64.10. *2003 Abstract Viewer/Itinerary Planner*. Society for Neuroscience, Washington, DC.

Nagy, I. & Woolf, C.J. (1996) Lignocaine selectively reduces C fibre-evoked neuronal activity in rat spinal cord in vitro by decreasing *N*-methyl-D-aspartate and neurokinin receptor-mediated post-synaptic depolarizations; implications for the development of novel centrally acting analgesics. *Pain*, **64**, 59-70.

Naim, M., Spike, R.C., Watt, C., Shehab, S.A. & Todd, A.J. (1997) Cells in laminae III and IV of the rat spinal cord that possess the neurokinin-1 receptor and have dorsally directed dendrites receive a major synaptic input from tachykinin-containing primary afferents. *J Neurosci*, **17**, 5536-5548.

Nilsson, H.J. & Schouenborg, J. (1999) Differential inhibitory effect on human nociceptive skin senses induced by local stimulation of thin cutaneous fibers. *Pain*, **80**, 103-112.

Ottersen, O.P. (1989) Quantitative electron microscopic immunocytochemistry of neuroactive amino acids. *Anat Embryol (Berl)*, **180**, 1-15.

Ouyang, Y., Kantor, D., Harris, K.M., Schuman, E.M. & Kennedy, M.B. (1997) Visualization of the distribution of autophosphorylated calcium/calmodulin-dependent protein kinase II after tetanic stimulation in the CA1 area of the hippocampus. *J Neurosci*, **17**, 5416-5427.

Petersen, J.D., Chen, X., Vinade, L., Dosemeci, A., Lisman, J.E. & Reese, T.S. (2003) Distribution of postsynaptic density (PSD)-95 and $Ca^{2+}$/calmodulin-dependent protein kinase II at the PSD. *J Neurosci*, **23**, 11270-11278.

Poncer, J.C., Esteban, J.A. & Malinow, R. (2002) Multiple mechanisms for the potentiation of AMPA receptor-mediated transmission by $\alpha$-$Ca^{2+}$/calmodulin-dependent protein kinase II. *J Neurosci*, **22**, 4406-4411.

Ralston, H.J., 3rd & Ralston, D.D. (1979) The distribution of dorsal root axons in laminae I, II and III of the macaque spinal cord: a quantitative electron microscope study. *J Comp Neurol*, **184**, 643-684.

Randic, M., Jiang, M.C. & Cerne, R. (1993) Long-term potentiation and long-term depression of primary afferent neurotransmission in the rat spinal cord. *J Neurosci*, **13**, 5228-5241.

Ribeiro-da-Silva, A. & Coimbra, A. (1982) Two types of synaptic glomeruli and their distribution in laminae I-III of the rat spinal cord. *J Comp Neurol*, **209**, 176-186.

Rodrigues, S.M., Farb, C.R., Bauer, E.P., LeDoux, J.E. & Schafe, G.E. (2004) Pavlovian fear conditioning regulates $Thr^{286}$ autophosphorylation of $Ca^{2+}$/calmodulin-dependent protein kinase II at lateral amygdala synapses. *J Neurosci*, **24**, 3281-3288.

Sandkühler, J. (2000) Learning and memory in pain pathways. *Pain*, **88**, 113-118.

Sandkühler, J., Chen, J.G., Cheng, G. & Randic, M. (1997) Low-frequency stimulation of afferent Aδ-fibers induces long-term depression at primary afferent synapses with substantia gelatinosa neurons in the rat. *J Neurosci*, **17**, 6483-6491.

Sandkühler, J. & Liu, X. (1998) Induction of long-term potentiation at spinal synapses by noxious stimulation or nerve injury. *Eur J Neurosci*, **10**, 2476-2480.

Schweitzer, E.S., Sanderson, M.J. & Wasterlain, C.G. (1995) Inhibition of regulated catecholamine secretion from PC12 cells by the $Ca^{2+}$/calmodulin kinase II inhibitor KN-62. *J Cell Sci*, **108 ( Pt 7)**, 2619-2628.

Shen, K. & Meyer, T. (1999) Dynamic control of CaMKII translocation and localization in hippocampal neurons by NMDA receptor stimulation. *Science*, **284**, 162-167.

Shen, K., Teruel, M.N., Connor, J.H., Shenolikar, S. & Meyer, T. (2000) Molecular memory by reversible translocation of calcium/calmodulin-dependent protein kinase II. *Nat Neurosci*, **3**, 881-886.

South, S.M., Kohno, T., Kaspar, B.K., Hegarty, D., Vissel, B., Drake, C.T., Ohata, M., Jenab, S., Sailer, A.W., Malkmus, S., Masuyama, T., Horner, P., Bogulavsky, J., Gage, F.H., Yaksh, T.L., Woolf, C.J., Heinemann, S.F. & Inturrisi, C.E. (2003) A conditional deletion of the NR1 subunit of the NMDA receptor in adult spinal cord dorsal horn reduces NMDA currents and injury-induced pain. *J Neurosci*, **23**, 5031-5040.

Strack, S., Choi, S., Lovinger, D.M. & Colbran, R.J. (1997) Translocation of autophosphorylated calcium/calmodulin-dependent protein kinase II to the postsynaptic density. *J Biol Chem*, **272**, 13467-13470.

Stucky, C.L. & Lewin, G.R. (1999) Isolectin $B_4$-positive and -negative nociceptors are functionally distinct. *J Neurosci*, **19**, 6497-6505.

Svendsen, F., Tjølsen, A., Gjerstad, J. & Hole, K. (1999) Long term potentiation of single WDR neurons in spinalized rats. *Brain Res*, **816**, 487-492.

Svendsen, F., Tjølsen, A. & Hole, K. (1997) LTP of spinal Aβ and C-fibre evoked responses after electrical sciatic nerve stimulation. *Neuroreport*, **8**, 3427-3430.

Svendsen, F., Tjølsen, A. & Hole, K. (1998) AMPA and NMDA receptor-dependent spinal LTP after nociceptive tetanic stimulation. *Neuroreport*, **9**, 1185-1190.

Taha, S., Hanover, J.L., Silva, A.J. & Stryker, M.P. (2002) Autophosphorylation of αCaMKII is required for ocular dominance plasticity. *Neuron*, **36**, 483-491.

Terashima, T., Ochiishi, T. & Yamauchi, T. (1994) Immunohistochemical detection of calcium/calmodulin-dependent protein kinase II in the spinal cord of the rat and monkey with special reference to the corticospinal tract. *J Comp Neurol*, **340**, 469-479.

Todd, A.J. (1996) GABA and glycine in synaptic glomeruli of the rat spinal dorsal horn. *Eur J Neurosci*, **8**, 2492-2498.

Todd, A.J., Hughes, D.I., Polgar, E., Nagy, G.G., Mackie, M., Ottersen, O.P. & Maxwell, D.J. (2003) The expression of vesicular glutamate transporters VGLUT1 and VGLUT2 in neurochemically defined axonal populations in the rat spinal cord with emphasis on the dorsal horn. *Eur J Neurosci*, **17**, 13-27.

Todd, A.J., Puskar, Z., Spike, R.C., Hughes, C., Watt, C. & Forrest, L. (2002) Projection neurons in lamina I of rat spinal cord with the neurokinin 1 receptor are selectively innervated by substance P-containing afferents and respond to noxious stimulation. *J Neurosci*, **22**, 4103-4113.

Tominaga, M., Caterina, M.J., Malmberg, A.B., Rosen, T.A., Gilbert, H., Skinner, K., Raumann, B.E., Basbaum, A.I. & Julius, D. (1998) The cloned capsaicin receptor integrates multiple pain-producing stimuli. *Neuron*, **21**, 531-543.

Valtschanoff, J.G., Phend, K.D., Bernardi, P.S., Weinberg, R.J. & Rustioni, A. (1994) Amino acid immunocytochemistry of primary afferent terminals in the rat dorsal horn. *J Comp Neurol*, **346**, 237-252.

Wang, X., Butowt, R., Vasko, M.R. & von Bartheld, C.S. (2002) Mechanisms of the release of anterogradely transported neurotrophin-3 from axon terminals. *J Neurosci*, **22**, 931-945.

Vikman, K.S., Kristensson, K. & Hill, R.H. (2001) Sensitization of dorsal horn neurons in a two-compartment cell culture model: wind-up and long-term potentiation-like responses. *J Neurosci*, **21**, RC169.

Willis, W.D. (2002) Long-term potentiation in spinothalamic neurons. *Brain Res Brain Res Rev*, **40**, 202-214.

Woolf, C.J. & Salter, M.W. (2000) Neuronal plasticity: increasing the gain in pain. *Science*, **288**, 1765-1769.

Vulchanova, L., Riedl, M.S., Shuster, S.J., Stone, L.S., Hargreaves, K.M., Buell, G., Surprenant, A., North, R.A. & Elde, R. (1998) $P2X_3$ is expressed by DRG neurons that terminate in inner lamina II. *Eur J Neurosci*, **10**, 3470-3478.

Zhabotinsky, A.M. (2000) Bistability in the $Ca^{2+}$/calmodulin-dependent protein kinase-phosphatase system. *Biophys J*, **79**, 2211-2221.

Zhang, Y. & Lipton, P. (1999) Cytosolic $Ca^{2+}$ changes during in vitro ischemia in rat hippocampal slices: major roles for glutamate and $Na^{+}$-dependent $Ca^{2+}$ release from mitochondria. *J Neurosci*, **19**, 3307-3315.

**Table 1. Postembedding immunogold labeling of pCaMKII in single sections through postsynaptic densities of primary afferent synapses**

| | | | | Statistical significance[1] | | |
|---|---|---|---|---|---|---|
| | **Rat 1** | **Rat 2** | **Rat 3** | **vs I** | **vs II** | **vs III** |
| **Average tissue labeling ($\mu m^{-2}$)** | 4.3 | 3.4 | 6.6 | | | |
| **Area labeling density ($\mu m^{-2}$)** | | | | | | |
| **I. DSA** | 62.3 | 71.7 | 163.2 | - | | |
| **II. SP/CGRP** | 51.7 | 26.8 | 126.5 | | - | |
| **III. LTM** | 42.2 | 29.1 | 82.0 | | | - |
| **Frequency of immunopositive PSDs (*n*)** | | | | | | |
| **I. DSA** | 72% (39) | 55% (74) | 87% (84) | - | | ** |
| **II. SP/CGRP** | 51% (41) | 39% (44) | 82% (78) | | - | * |
| **III. LTM** | 37% (95) | 19% (73) | 51% (71) | ** | * | - |

Average tissue labeling is the pooled gold particle density in 10 random electron micrographs (mean sampled area in each micrograph, 23 $\mu m^2$) of the superficial dorsal horn. Area labeling density is the number of gold particles lying immediately over the postsynaptic density (PSD) per $\mu m^2$ of PSD cross sectional area. Frequency of immunopositive PSDs is the proportion of PSDs with at least one gold particle lying no more than 25 nm from the PSD. **DSA**, synapses formed by dense sinusoid axon terminals; **SP/CGRP**, synapses formed by terminals containing substance P and calcitonin gene-related peptide; **LTM**, synapses formed by presumed low-threshold mechanosensitive primary afferent fiber terminals. [1]Repeated measures ANOVA followed by Tukey's post hoc test; $^{**}P < 0.01$; $^{*}P < 0.05$.

**Table 2. Linear densities of pCaMKII immunogold labeling at primary afferent synapses**

| | | | | Statistical significance[1] | | |
|---|---|---|---|---|---|---|
| | **Rat 1** | **Rat 2** | **Rat 3** | **vs I** | **vs II** | **vs III** |
| **All synapses** | | | | | | |
| **I. DSA** | 4.6 | 4.4 | 9.9 | - | | * |
| **II. SP/CGRP** | 3.2 | 1.8 | 8.0 | | - | |
| **III. LTM** | 2.3 | 1.2 | 5.0 | * | | - |
| **Immunopositive synapses** | | | | | | |
| **I. DSA** | 6.0 | 7.2 | 11.1 | - | | |
| **II. SP/CGRP** | 5.2 | 4.9 | 9.3 | | - | |
| **III. LTM** | 5.6 | 5.7 | 8.4 | | | - |

Linear labeling density is the number of gold particles associated with the postsynaptic density per μm of postsynaptic membrane. **DSA**, synapses formed by dense sinusoid axon terminals; **SP/CGRP**, synapses formed by terminals containing substance P and calcitonin gene-related peptide; **LTM**, synapses formed by presumed low-threshold mechanosensitive primary afferent fiber terminals. [1]Repeated measures ANOVA followed by Tukey's post hoc test; $*P < 0.05$.

**Table 3. Presynaptic immunogold labeling of pCaMKII**

| | Rat 1 | Rat 2 | Rat 3 |
|---|---|---|---|
| **DSA** | 1.5 | 3.4 | 2.5 |
| **SP/CGRP** | 1.4 | 2.4 | 2.1 |
| **LTM** | 1.3 | 1.4 | 2.1 |

Shown is the ratio between axoplasmic gold particle density (in the presynaptic region between the lateral borders of the synapse and within 10–100 nm of the postsynaptic membrane) and average tissue immunolabeling density for each rat (see Table 1). **DSA**, dense sinusoid axon terminals; **SP/CGRP**, terminals containing substance P and calcitonin gene-related peptide; **LTM**, presumed low-threshold mechanosensitive primary afferent fiber terminals.

## Figure legends

**Figure 1.** Immunolabeling of pCaMKII in the dorsal horn. **A**, photomicrograph of lumbar dorsal horn (laminae I–V) immunoperoxidase labeled for pCaMKII. Laminar borders (dashed lines) were delineated according to Molander et al. (1984). **B**, electron micrograph of pCaMKII immunoperoxidase labeled dorsal horn, showing a dense sinusoid axon terminal (DSA) forming two synapses with conspicuous reaction product associated with their postsynaptic density (arrowheads). An unidentified terminal (T) forms an immunoreactive synapse with a dendrite (D) which also exhibits dense cytosolic immunolabeling. **C**, a glomerular terminal of presumed low-threshold primary afferent origin (LTM) forming two distinctly immunoreactive synapses (arrowheads), as well as one less evidently labeled synapse (arrow). Some reaction product appears to be associated with presynaptic active zones. Scale bar in A, 200 μm; scale bar in C, 250 nm, valid for B and C.

**Figure 2.** Effects on basal pCaMKII immunolabeling of ischemia or neuronal activity blockade during aldehyde fixation. **A**, pCaMKII immunofluorescence in the dorsal horn from animals perfused with rinsing buffer for 30 s (left panel) or 90 s (right panel) prior to fixative administration. **B**, pCaMKII immunolabeled sections from spinal cord slices incubated in the absence (left panel) or presence (right panel) of TTX prior to and during fixation. **C**, pCaMKII immunolabeling of dorsal horn from rats perfused with normal rinsing buffer (left panel) or buffer containing 3 mM lidocaine (right panel) prior to fixation. Scale bar in C is 200 μm, valid for all panels.

**Figure 3.** Postembedding immunogold labeling of pCaMKII in synapses formed by dense sinusoid axon terminals (DSAs). **$A_1$**, a DSA forming several synapses with immunopositive postsynaptic densities, two of which are shown in this micrograph (indicated by arrow and arrowhead). **$A_2$**, the same terminal as in $A_1$, shown at lower

magnification, in the adjacent non-immunogold labeled section. Arrow and arrowhead indicate the same synapses as in $A_1$. **B, C** show two examples of immunolabeled synapse. Inset in B shows the synapse at lower magnification in the adjacent non-labeled section; arrowheads in B and inset indicate an immunolabeled multivesicular body. **D** and **E** show two DSAs forming multiple immunopositive synapses. Scale bar in D is 150 nm, for $A_1$, B, C and D. Scale bar in E is 250 nm, valid for $A_2$, E and inset in B.

**Figure 4.** pCaMKII immunogold labeling of synapses formed by terminals containing substance P (SP) and calcitonin gene-related peptide (CGRP). $\mathbf{A_1}$, $\mathbf{B_1}$ and $\mathbf{C_1}$ show immunolabeling of pCaMKII, whereas $\mathbf{A_2}$, $\mathbf{B_2}$ and $\mathbf{C_2}$ show immunolabeling of SP (5 nm gold) and CGRP (15 nm gold) in the adjacent sections. Note the immunogold labeling over presynaptic axoplasm in $C_1$. Scale bar in $C_2$ is 150 nm, valid for all panels.

**Figure 5.** pCaMKII immunogold labeling of synapses formed by presumed low-threshold mechanosensitive primary afferent fiber terminals (LTMs). $\mathbf{A_1}$, $\mathbf{A_2}$ show in a pCaMKII labeled section ($A_1$) and in a consecutive non-labeled section ($A_2$) a morphologically typical LTM, exhibiting one immunopositive (arrow) and one immunonegative synapse (arrowhead). **B**, **C**, two additional examples of LTM forming immunolabeled and non-labeled synapses. Scale bar in B is 150 nm, valid for $A_1$ and B. Scale bar in C is 250 nm, valid for $A_2$ and C.

**Figure 6.** Presence of pCaMKII immunogold labeling in postsynaptic densities postsynaptic to primary afferent terminals. Shown are histograms of immunolabeled synapses formed by dense sinusoid axon terminals (DSA), terminals containing substance P and calcitonin gene-related peptide (SP/CGRP), and terminals of

presumed low-threshold primary afferent origin (LTM) in each of the rats examined. Gold particles were included if they were within 25 nm of the postsynaptic density.

**Figure 7.** Immunogold labeling of pCaMKII in serially sectioned synapses. **A**, fraction of DSA or LTM synapses lacking pCaMKII-like immunoreactivity in one or more of three consecutive sections. **B**, summed linear density of pCaMKII immunogold label in three serial sections (total no. of gold particles in the three sections divided by summed postsynaptic membrane length) through DSA and LTM synapses. Error bars indicate SD. $^{**}P = 0.002$ (Student's *t* test).

**Figure 8.** Axodendritic distribution of immunogold labeling of pCaMKII in primary afferent synapses. Only gold particles within the lateral borders of the synapse and within 100 nm of the postsynaptic membrane were included (gold particles from all rats were pooled). Gold particles were placed in 10 nm bins with respect to their distance to the outer surface of the postsynaptic membrane. The distances to the postsynaptic membrane of presynaptic gold particles and of gold particles within the synaptic cleft were negated. Dashed lines indicate average tissue labeling in laminae I–II.

**Figure 9.** Histogram of the distances of gold particles associated with the PSD along the mediolateral axis to the center of the synapse. Distances were normalized, 0 indicating the center and 1 the lateral border of the synapse. Only gold particles associated with synapses larger than 200 nm were included.

**Figure 10.** Association of pCaMKII-like immunoreactivity with dense core vesicles in SP/CGRP terminals. **A**, part of a SP/CGRP-positive terminal exhibiting pCaMKII immunogold labeling associated with dense core vesicles (DCVs). Scale bar, 100 nm. **B**, distribution of the distance to the center of the nearest DCV of pCaMKII immunogold label (bars) and of random points (solid line). The spatial distribution of

gold particles relative to DCVs was significantly different from that of random points versus DCVs ($P < 0.0001$, $\chi^2$ test). Indicated is also the distribution of DCV radii (dashed line).

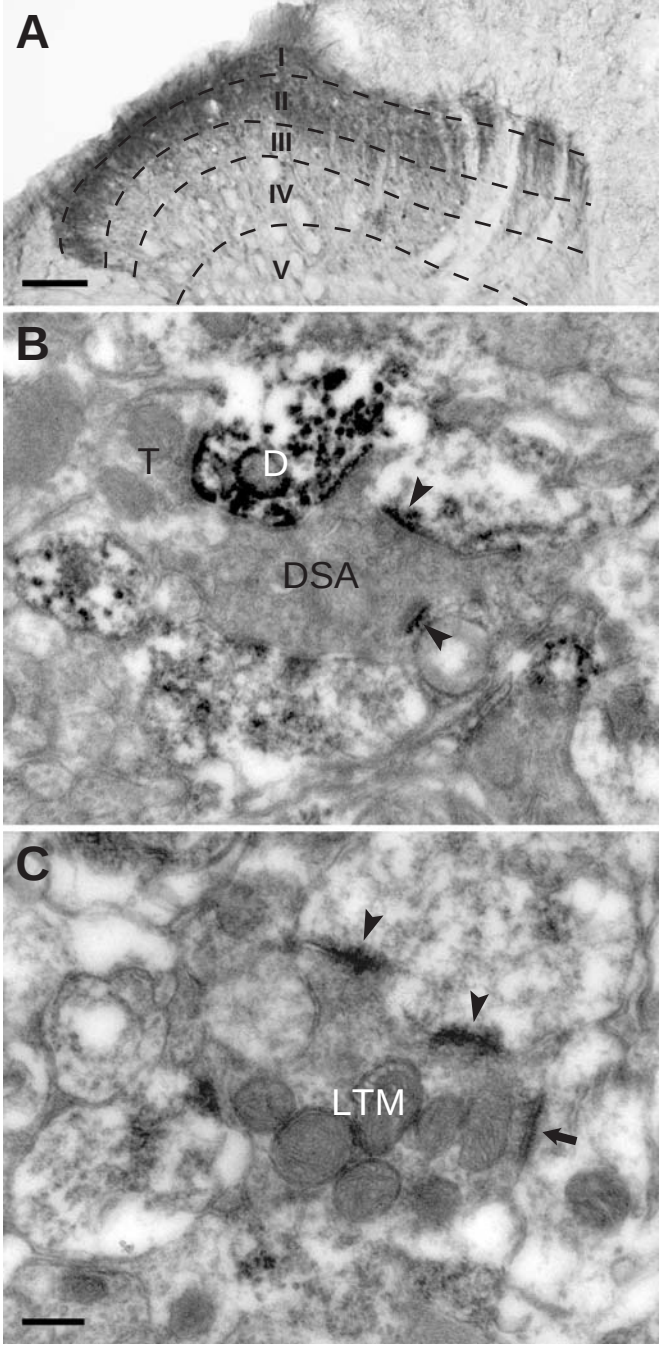


# Figure 1

Larsson M, Broman J. Different basal levels of CaMKII phosphorylated at Thr$^{286/287}$ at nociceptive and low threshold primary afferent synapses

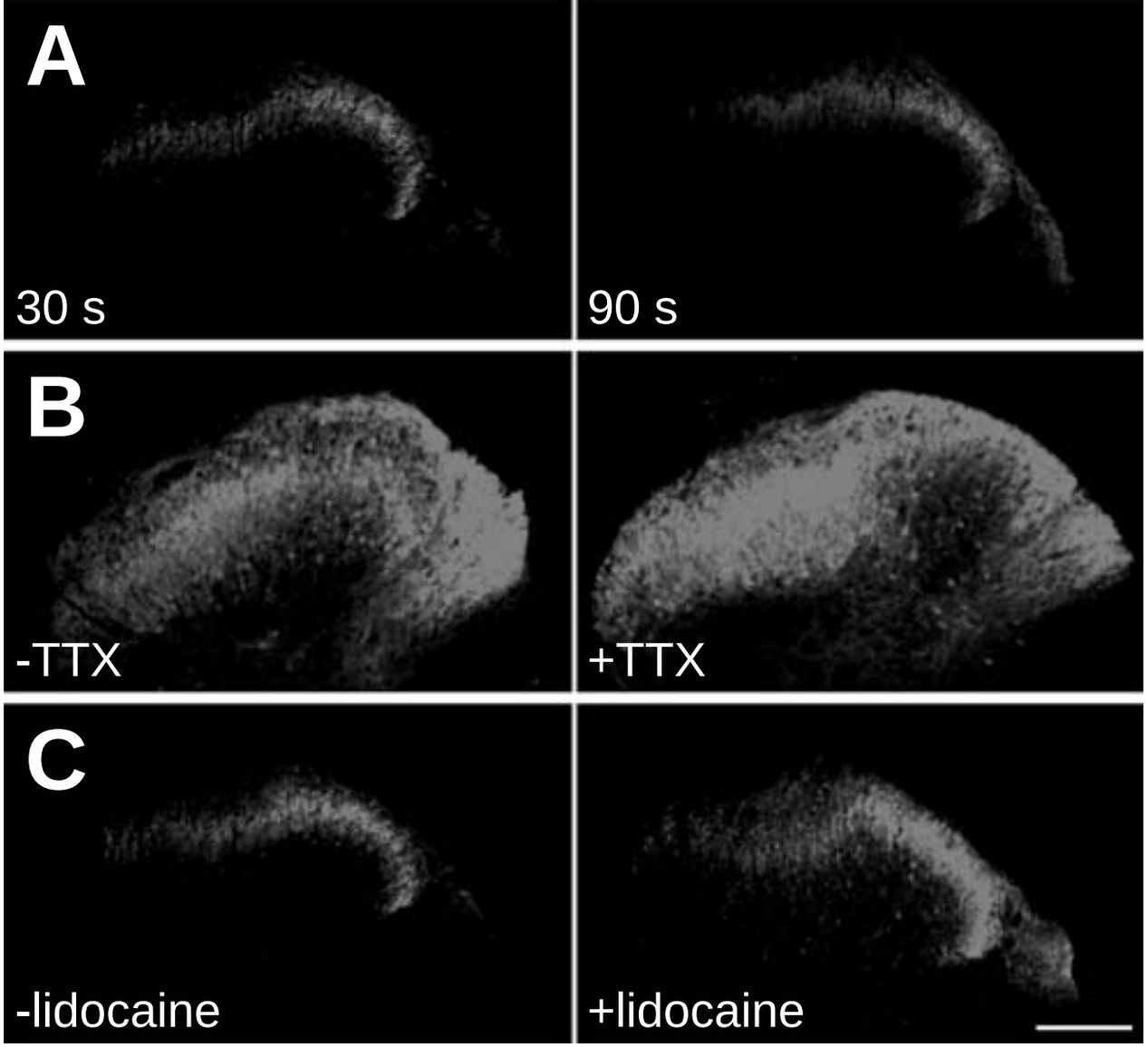


# Figure 2

Larsson M, Broman J. Different basal levels of CaMKII phosphorylated at Thr$^{286/287}$ at nociceptive and low threshold primary afferent synapses

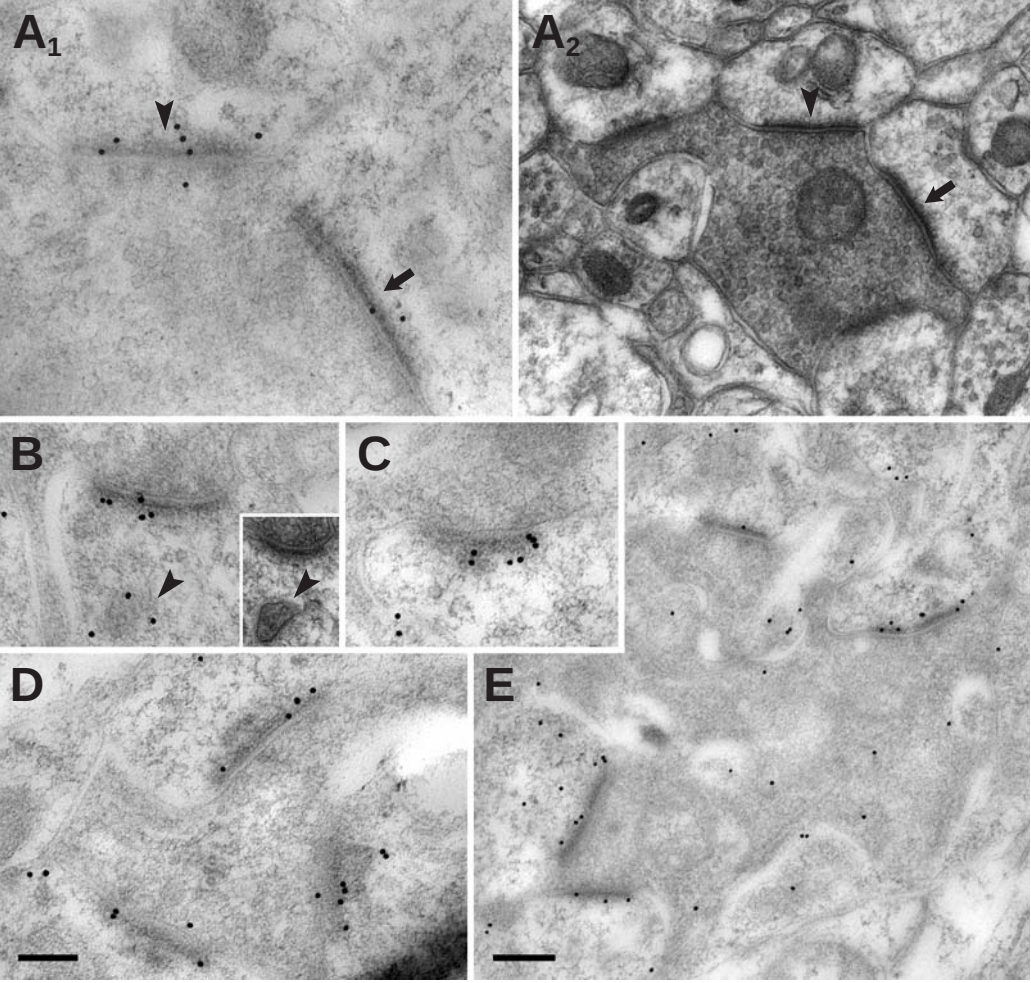


# Figure 3

Larsson M, Broman J. Different basal levels of CaMKII phosphorylated at Thr$^{286/287}$ at nociceptive and low threshold primary afferent synapses

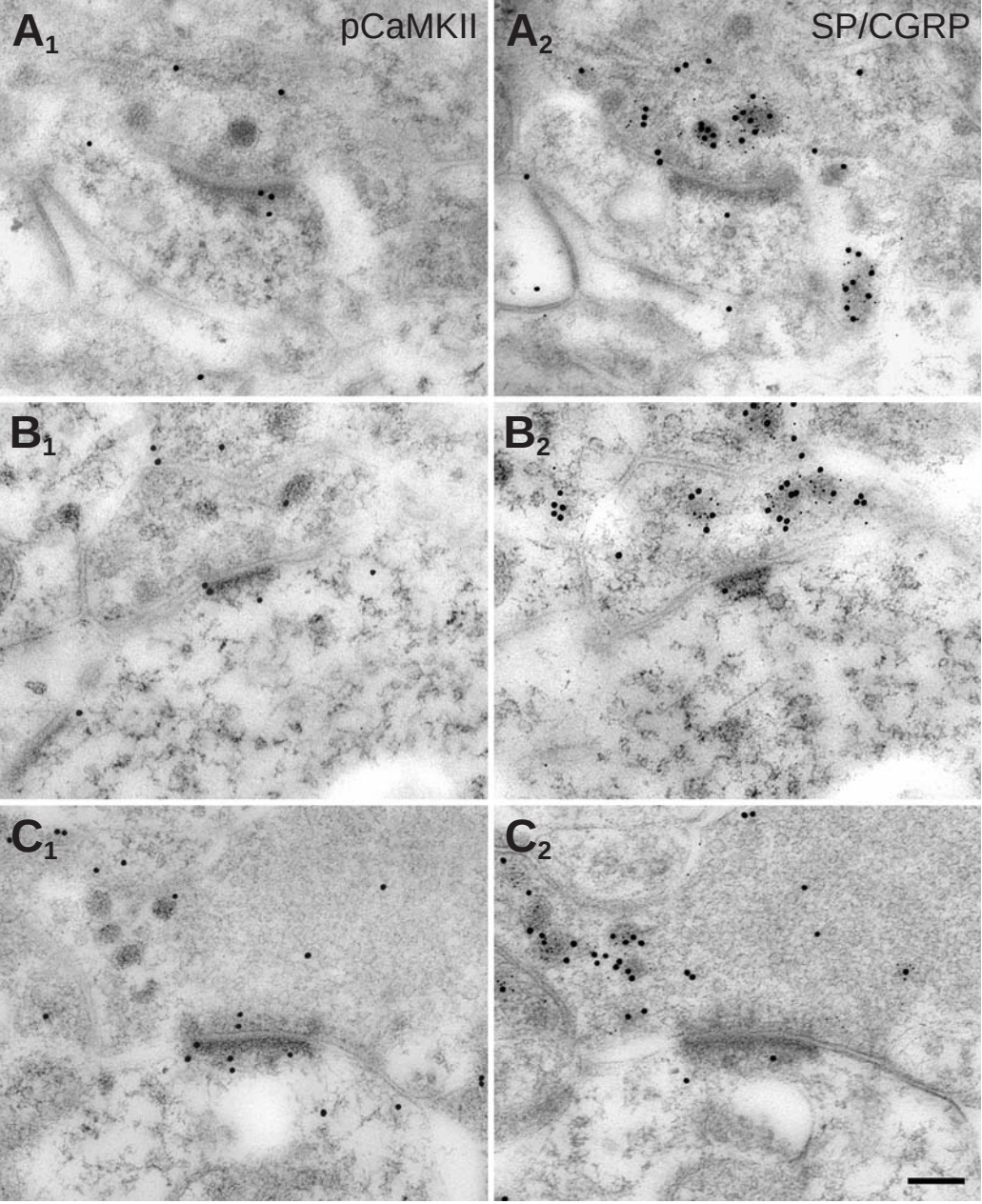


# Figure 4

Larsson M, Broman J. Different basal levels of CaMKII phosphorylated at $Thr^{286/287}$ at nociceptive and low threshold primary afferent synapses

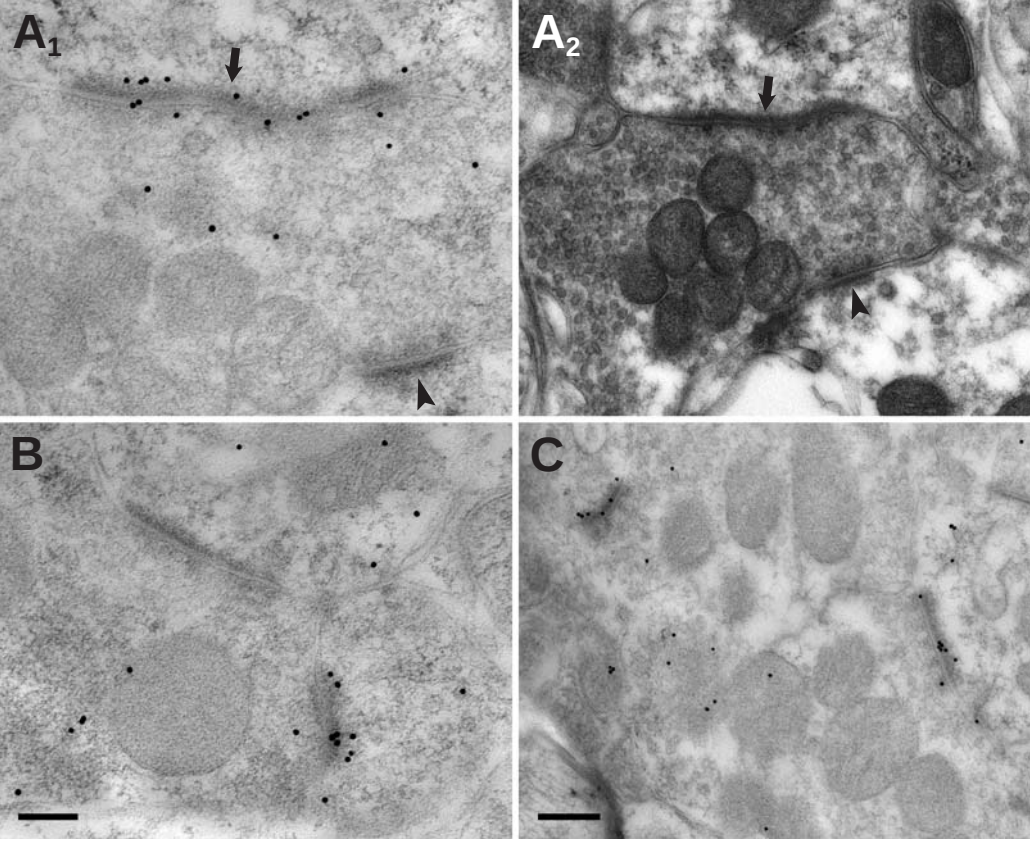


# Figure 5

Larsson M, Broman J. Different basal levels of CaMKII phosphorylated at Thr$^{286/287}$ at nociceptive and low threshold primary afferent synapses

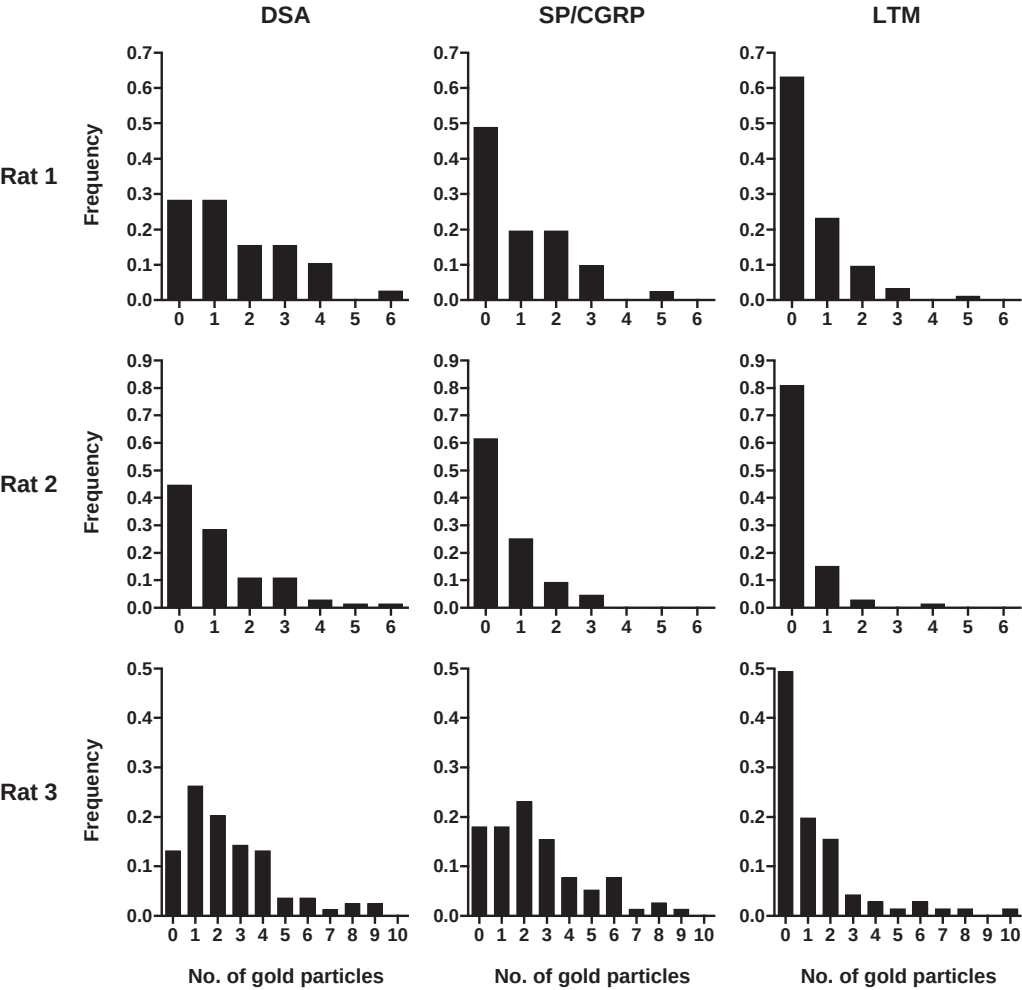


# Figure 6

Larsson M, Broman J. Different basal levels of CaMKII phosphorylated at Thr$^{286/287}$ at nociceptive and low threshold primary afferent synapses

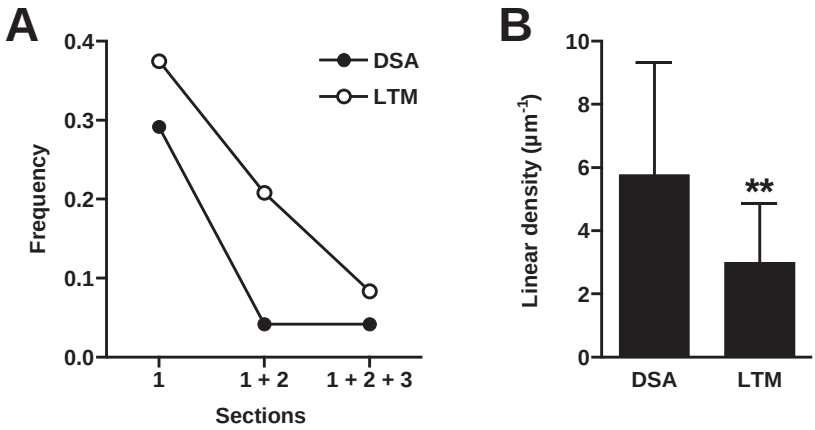


# Figure 7

Larsson M, Broman J. Different basal levels of CaMKII phosphorylated at Thr$^{286/287}$ at nociceptive and low threshold primary afferent synapses

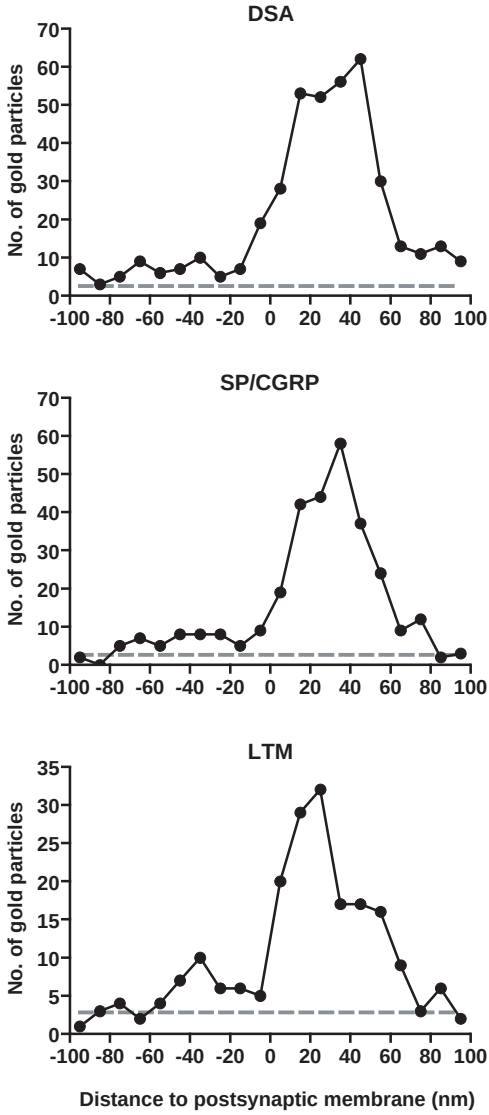


# Figure 8

Larsson M, Broman J. Different basal levels of CaMKII phosphorylated at Thr$^{286/287}$ at nociceptive and low threshold primary afferent synapses

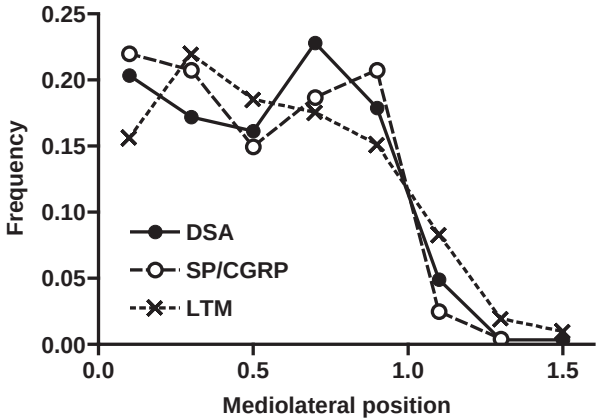


# Figure 9

Larsson M, Broman J. Different basal levels of CaMKII phosphorylated at Thr$^{286/287}$ at nociceptive and low threshold primary afferent synapses

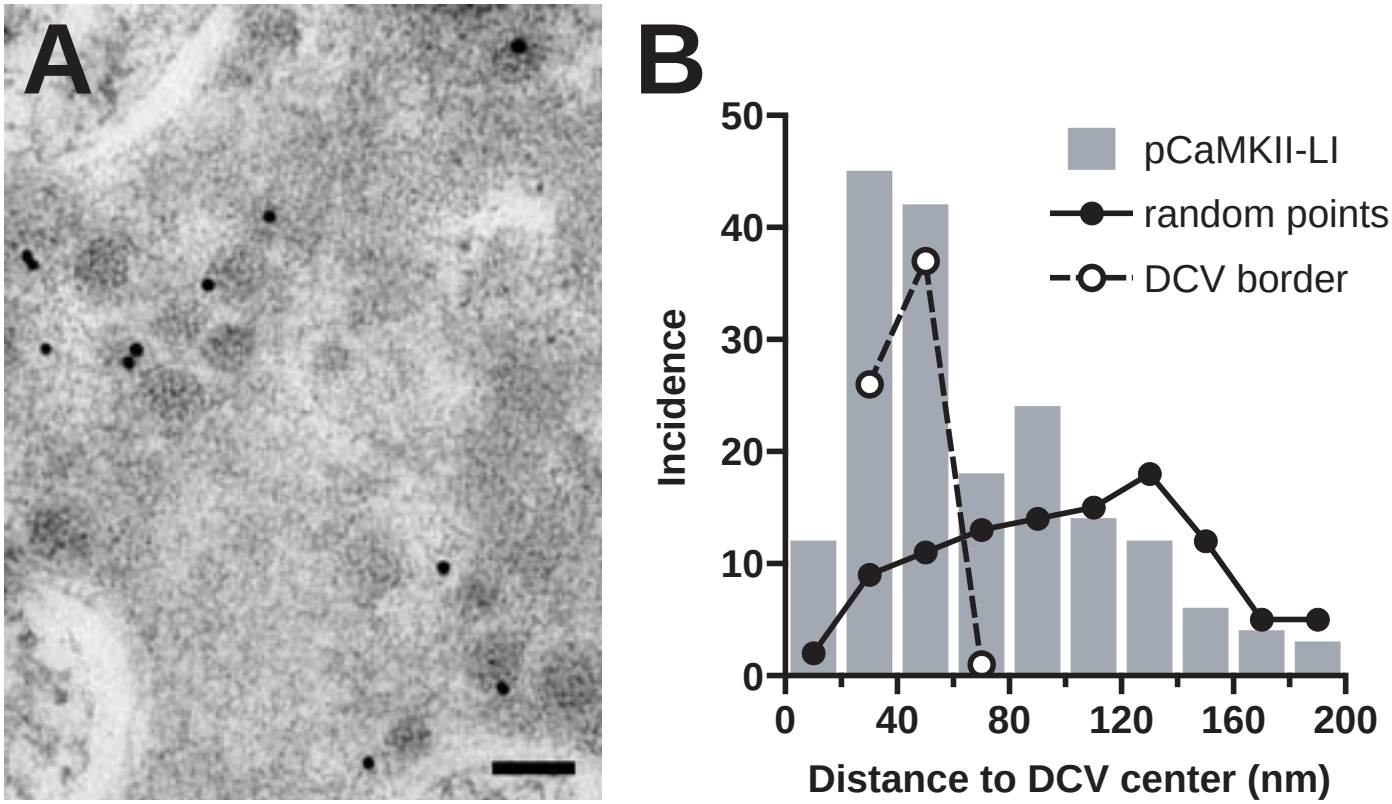


# Figure 10

Larsson M, Broman J. Different basal levels of CaMKII phosphorylated at Thr$^{286/287}$ at nociceptive and low threshold primary afferent synapses